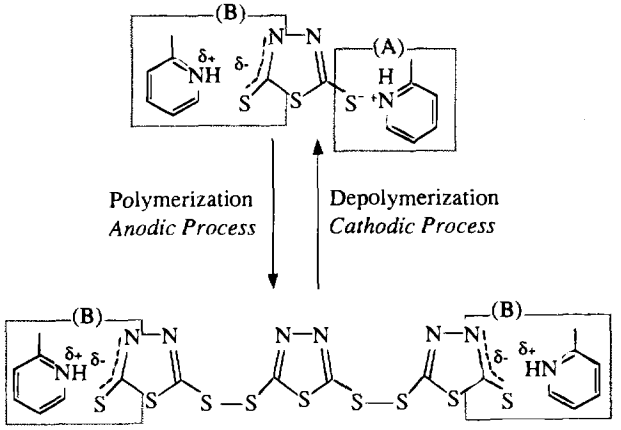

Fig. 5. Proposed structural change of DMcT in PVP film during the oxidation-reduction cycle.

the drawbacks previously mentioned for DMcT electrodes have been overcome by using DMcT/PVP composite films.

Acknowledgment

The present work has been financially supported by the Japanese Ministry of Education. K.N. would like to thank Mitsubishi Chemicals for supplying high quality PC solvent.

Manuscript submitted June 19, 1996; revised manuscript received about Dec. 5, 1996.

Tokyo University of Agriculture and Technology assisted in meeting the publication costs of this article.

REFERENCES

1. S. J. Visco and L. C. DeJonghe, in *Handbook of Solid State Batteries and Capacitors*, M. Z. A. Munshi, Editor, Chap. 22, World Scientific, NJ (1995).
2. K. Naoi, M. Menda, H. Ooike, and N. Oyama, *J. Electroanal. Chem.*, **318,** 395 (1992).
3. A. Kaminaga, T. Tatsuma, T. Sotomura, and N. Oyama, *This Journal,* **142,** L47 (1995).
4. N. Oyama, T. Tatsuma, T. Sato, and T. Sotomura, *Nature,* **373,** 598 (1995).
5. J. M. Liu, S. J. Visco, and L. C. DeJonghe, *This Journal,* **136,** 2570 (1989).
6. J. M. Liu, S. J. Visco, and L. C. DeJonghe, *ibid.*, **138,** 1891 (1991).
7. J. M. Liu, S. J. Visco, and L. C. DeJonghe, *ibid.*, **138,** 1896 (1991).
8. T. Sotomura, H. Uemachi, K. Takehara, K. Naoi, and N. Oyama, *Electrochim. Acta,* **37,** 1851 (1992).
9. Y. Iwamizu, Y. Oura, and K. Naoi, in *Proceedings of 36th Japanese Battery Meeting,* p. 51 (1995).
10. I. Sekine, K. Kohara, T. Sugiyama, and M. Yuasa, *This Journal,* **139,** 3090 (1992).
11. K. Naoi, Y. Oura, Y. Iwamizu, and N. Oyama, *ibid.*, **142,** 354 (1995).
12. S. Picart and E. Genies, *J. Electroanal. Chem.*, **53,** 408 (1996).
13. G. D. Thorn, *Can. J. Chem.*, **38,** 1439 (1960).
14. B. Stanovnik and M. Tisler, *Croat. Chem. Acta,* **37,** 17 (1965).
15. A. J. Bard and L. R. Faulkner, in *Electrochemical Methods, Fundamentals and Applications,* Chap. 3, John Wiley & Sons, Inc., New York (1980).
16. E. M. Genies and S. Picart, *Synth. Met.*, **69,** 165 (1995).
17. M. Mori, Y. Naruoka, W. Kokubo, and K. Naoi, in 1996 Japanese Electrochemical Society Autumn Meeting, p. 16 (1996).

Phospho-olivines as Positive-Electrode Materials for Rechargeable Lithium Batteries

A. K. Padhi,* K. S. Nanjundaswamy, and J. B. Goodenough**

Center for Materials Science and Engineering, The University of Texas at Austin, Austin, Texas 78712-1063, USA

ABSTRACT

Reversible extraction of lithium from $LiFePO_4$ (triphylite) and insertion of lithium into $FePO_4$ at 3.5 V *vs.* lithium at 0.05 mA/cm^2 shows this material to be an excellent candidate for the cathode of a low-power, rechargeable lithium battery that is inexpensive, nontoxic, and environmentally benign. Electrochemical extraction was limited to ~0.6 Li/formula unit; but even with this restriction the specific capacity is 100 to 110 mAh/g. Complete extraction of lithium was performed chemically; it gave a new phase, $FePO_4$, isostructural with heterosite, $Fe_{0.65}Mn_{0.35}PO_4$. The $FePO_4$ framework of the ordered olivine $LiFePO_4$ is retained with minor displacive adjustments. Nevertheless the insertion/extraction reaction proceeds via a two-phase process, and a reversible loss in capacity with increasing current density appears to be associated with a diffusion-limited transfer of lithium across the two-phase interface. Electrochemical extraction of lithium from isostructural $LiMPO_4$ (M = Mn, Co, or Ni) with an $LiClO_4$ electrolyte was not possible; but successful extraction of lithium from $LiFe_{1-x}Mn_xPO_4$ was accomplished with maximum oxidation of the Mn^{3+}/Mn^{2+} occurring at $x = 0.5$. The Fe^{3+}/Fe^{2+} couple was oxidized first at 3.5 V followed by oxidation of the Mn^{3+}/Mn^{2+} couple at 4.1 V *vs.* lithium. The Fe^{3+}-O-Mn^{2+} interactions appear to destabilize the Mn^{2+} level and stabilize the Fe^{3+} level so as to make the Mn^{3+}/Mn^{2+} energy accessible.

Introduction

Since the demonstration of reversible lithium intercalation between the layers of TiS_2,[1] considerable effort has been devoted to the identification of other lithium-insertion compounds that can be used as the cathode for a secondary lithium battery. The desired material would have a relatively flat open-circuit voltage over a large lithium solid solution within the voltage range of $2.5 < V_{oc} < 4.0$ V and be inexpensive, easy to fabricate, environmentally benign, and safe in handling and operation. Reversible lithium insertion/extraction has been performed on a variety of compounds containing different transition-metal cations and structural architectures. The sulfides have too low a V_{oc} and the halides too low an electronic conductivity, so particular attention has been given to transition-metal oxides. These efforts have resulted in the development of rechargeable lithium batteries that now serve as state of the art power sources for consumer electronics.

Among the known Li-insertion compounds, the layered rock salt systems $Li_{1-x}CoO_2$,[2] $Li_{1-x}NiO_2$,[3] and the manganese-spinel framework system $Li_{1-x}[Mn_2]O_4$[4] are now

* Electrochemical Society Student Member.
** Electrochemical Society Active Member.

used commercially as 4.0 V positive-electrode materials in rechargeable lithium batteries. However, the voltages in excess of 4.0 V on higher charge in these oxides can lead to the decomposition of the electrolytes, and the fully charged compounds are metastable: $[Mn_2]O_4$ converts to ϵ-MnO_2 at 190°C[5] while fully charged phases of $Li_{1-x}CoO_2$ and $Li_{1-x}NiO_2$ lose O_2 above 180 and 250°C, respectively.[6] Moreover, a lower lithium mobility within the $[Mn_2]O_4$ spinel framework limits its power capability. Although the $Li_{1+x}[Mn_2]O_4$ system has a flat $V_{oc} \approx 3.0$ V *vs.* lithium, which is attractive,[7] structural changes associated with a cooperative Jahn-Teller deformation of the framework tend to reduce the capacity irreversibly on repeated cycling.[8] In addition, the availability and cost of the transition metals used in these compounds are unfavorable as the Wh/$ is a more important figure of merit than Wh/g in the case of large batteries to be used in an electric vehicle or a load-leveling system. These consideration have motivated the investigations of iron-based oxides.

The iron-based oxides containing O^{2-} as the anion pose a problem for the cathode designer; in these oxides the Fe^{4+}/Fe^{3+} redox energy tends to lie too far below the Fermi energy of a lithium anode and the Fe^{3+}/Fe^{2+} couple too close to it. Layered $LiFeO_2$ prepared by ion-exchange from α-$NaFeO_2$ [9] has been investigated.[10] It would operate on the Fe^{4+}/Fe^{3+} redox couple, but it is metastable and gives unimpressive battery performance. The other iron-based compounds proposed, viz. $FePS_3$,[11] FeOCl,[12] and FeOOH,[13] have a relatively poor rechargeability and/or too low a discharge voltage. On the other hand, the use of polyanions such as $(SO_4)^{2-}$, $(PO_4)^{3-}$, $(AsO_4)^{3-}$, or even $(MoO_4)^{2-}$ or $(WO_4)^{2-}$ have been shown to lower the Fe^{3+}/Fe^{2+} redox energy to useful levels. Among the compounds with NASICON framework, for example, the open-circuit voltages *vs.* lithium are 3.6 V for $Li_xFe_2(SO_4)_3$,[14] 2.8 V for $Li_3Fe_2(PO_4)_3$,[15] and 2.75 V for $Li_2FeTi(PO_4)_3$ [16]; each of these materials has a specific capacity of about 100 mAh/g. Tuning of the energy of the Fe^{3+}/Fe^{2+} couple is accomplished through the choice of the countercation within the polyanion. Polarization of the electrons of the O^{2-} ions into strong covalent bonding within the polyanion reduces the covalent bonding to the iron ion, which lowers its redox energy. The stronger the covalent bonding within the polyanion, the lower is the Fe^{3+}/Fe^{2+} redox energy and the higher the V_{oc} *vs.* lithium for that couple.

The open NASICON framework allows fast Li^+-ion diffusion, but a separation of the FeO_6 octahedra by polyanions reduces the electronic conductivity, which is polaronic in the mixed-valent state. In this paper we report the cathode performance of an iron phosphate having an ordered olivine structure in which the FeO_6 octahedra share common corners.

The M_2XO_4 olivine structure has M atoms in half of the octahedral sites and X atoms in one-eighth of the tetrahedral sites of an hexagonal close-packed (hcp) oxygen array; it is the hexagonal analog of the cubic normal spinel $X[M_2]O_4$. Olivine crystallizes in preference to spinel for certain small X ions such as Be^{2+}, B^{3+}, Si^{4+}, P^{5+}, and occasionally Ge^{4+}. Unlike spinel, the two octahedral sites in olivine are crystallographically distinct and differ in size, which favors ordering in $MM'XO_4$ olivines containing M and M′ ions of different size and charge. The $LiMPO_4$ compounds, with M = Fe, Mn, Co, or Ni, have the ordered olivine structure.

Figure 1 shows the crystal structure of olivine: an ideal hcp model and the actual structure. In the actual structure, the M(1) site has $\bar{I}$ symmetry, the M(2) octahedron has mirror symmetry with average M-O distances greater than that in the M(1) octahedron. The M(1) sites form linear chains of edge-shared octahedra running parallel to the *c*-axis in the alternate *a*-*c* planes; the M(2) sites form zigzag planes of corner-shared octahedra running parallel to the *c*-axis in the other *a*-*c* planes (see Fig 6). Each M(1) site shares its edges with two M(2) sites and two X sites; there is one edge shared by an M(2) site with an X site.[17] Distortion of the hcp oxygen array has been related to the cation-cation coulomb repulsion across the shared edges. In the $LiMPO_4$ (M = Mn, Fe, Co, or Ni) compounds, the lithium moieties occupy M(1) sites and the M atoms M(2) sites. With Li in the continuous chain of edge-shared octahedra on alternate *a*-*c* planes, a reversible extraction/insertion of lithium from/into these chains would appear to be analogous to the two-dimensional extraction or insertion of lithium in the $LiMO_2$ layered oxides with M = Co or Ni. On the other hand, the XO_4 tetrahedra bridge between adjacent M(2) planes in the olivine structure, which constrains the free volume in which the Li^+-ions move; only the Li-O bonding constrains the spacing between MO_2 layers in the $LiMO_2$compounds.

Our attempts to delithiate $LiMnPO_4$, $LiCoPO_4$, and $LiNiPO_4$ proved unsuccessful with the $LiClO_4$ electrolyte used. However, we could use our ability to delithiate $LiFePO_4$ to initiate delithiation in the solid-solution system $LiFe_{1-x}Mn_xPO_4$; we report a Mn^{3+}/Mn^{2+} couple at

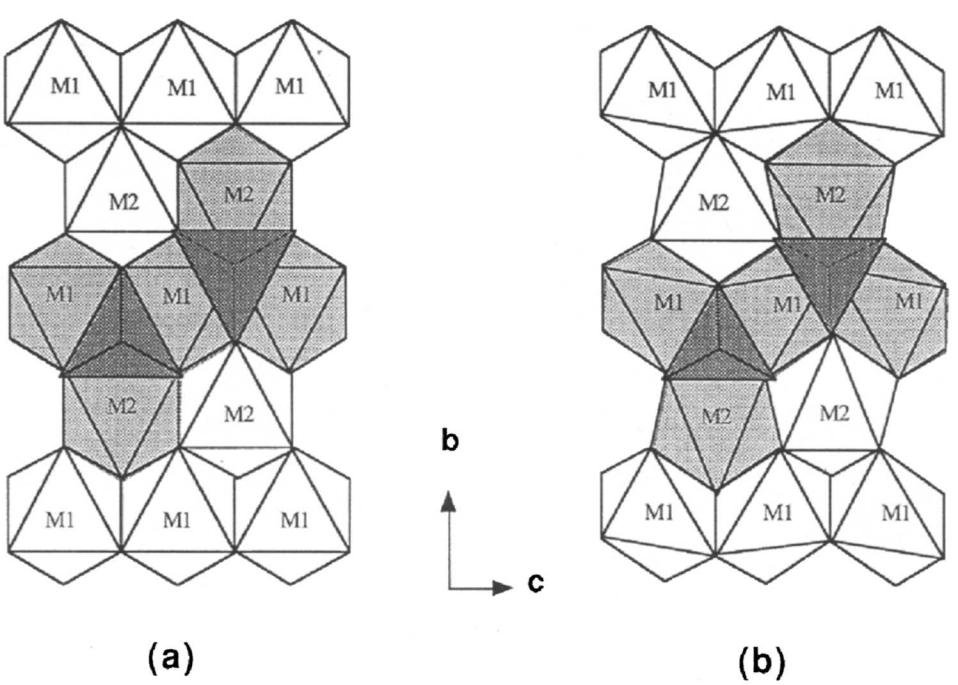

Fig. 1. Olivine crystal structure: (a) ideal HCP model, (b) actual stucture.

4.1 eV below the Fermi energy of a lithium anode where there are Fe^{3+}-O-Mn^{2+} interactions.

Experimental

$LiMPO_4$ (M = Mn, Fe, Co, or Ni) compounds were prepared by direct solid-state reaction of stoichiometric amounts of M(II)-acetates, ammonium phosphate, and lithium carbonate. $LiFePO_4$ and $LiFe_{1-x}Mn_xPO_4$ (x = 0.25, 0.50, and 0.75) were synthesized in inert atmosphere to prevent the formation of Fe^{3+} compounds as impurities. The intimately ground stoichiometric mixture of the starting materials was first decomposed at 300 to 350°C to drive away the gases. The mixture was then reground and returned to the furnace at 800°C for 24 h before being cooled slowly to room temperature. The x-ray powder diffraction technique was used to identify the phases. The unit-cell parameters were obtained with a least squares refinement to the diffraction peaks. Rietveld refinement of the x-ray diffraction (XRD) data was performed to obtain the structure.

The electrochemical extraction/insertion of lithium and characterization of the performance of the phospho-olivines as cathodes were made with coin-type cells (Type 2320). After the materials were ground to fine particles with a milling machine, they were mixed/blended with acetylene black and polytetrafluoroethylene (PTFE) in the weight ratio 70:25:5. This cathode mixture, after being kept at 140°C for 2 h, was rolled into thin sheets of uniform thickness and cut into pellets of required size for coin-cell fabrication. The electrolyte was 1 *M* $LiClO_4$ in a 1:1 mixture of propylene carbonate (PC) and dimethoxyethane (DME). A lithium foil was used as the anode. The coin cell was fabricated in a glove box under argon atmosphere.

Chemical delithiation to obtain $Li_{1-x}MPO_4$ ($0 < x < 1$) was performed by reacting the materials with nitronium hexafluorophosphate (NO_2PF_6) in acetonitrile under inert atmosphere. Reaction of $LiFePO_4$ with bromine in acetonitrile was also used to extract lithium chemically. Chemical lithiation was carried out by reacting the material with lithium iodide. The products were washed several times with acetonitrile to ensure the purity of the solid phase before it was dried in vacuum. Atomic absorption spectrosopy was performed on intermediate compositions to obtain the exact lithium content with a Perkin-Elmer 1100 spectrometer.

The thermal stability of the phases was monitored from 50 to 500°C by TGA and DSC techniques on a Perkin-Elmer Thermal Analysis 7 instrument. These experiments were performed in both oxygen and an inert atmosphere.

Results and Discussion

Electrochemical charge and discharge curves for $LiFePO_4$, Fig. 2, show that approximately 0.6 lithium atoms per formula unit can be extracted at a closed-circuit voltage of 3.5 V *vs.* lithium and the same amount can be reversibly inserted back into the structure on discharge. The extraction and insertion of lithium ions into the structure of $LiFePO_4$ is not only reversible on repeated cycling; the capacity actually increases slightly with cycling.

The placement of the Fe^{3+}/Fe^{2+} redox energy at 3.5 eV below the Fermi level of lithium in $Li_{1-x}FePO_4$ is to be compared with 2.8 eV found[15,16] in $Li_{3+x}Fe_2(PO_4)_3$ and $Li_{2+x}FeTi(PO_4)_3$ and at 3.6 eV in $Li_xFe_2(SO_4)_3$.[14] A difference of 0.8 eV between the redox energies in the isostructural NASICON frameworks of $Li_{3+x}Fe_2(PO_4)_3$ and $Li_xFe_2(SO_4)_3$ can be attributed to the inductive effect, the oxygen forming a stronger bond within $(SO_4)^{2-}$ than in $(PO_4)^{3-}$polyanions. On the other hand, all the oxygen of both $Li_{1-x}FePO_4$ and $Li_{3+x}Fe_2(PO_4)_3$ form strong covalent bonds within a $(PO_4)^{3-}$ complex, so the 0.7 eV difference in the Fe^{3+}/Fe^{2+} redox energies of these two compounds must have another origin than the inductive effect. For the origin of this difference, we turn to the ionic component of the bonding.

In an ionic compound, the position of the electron energy levels depends critically on the Madelung potential at the different atoms, which depends on both the structure

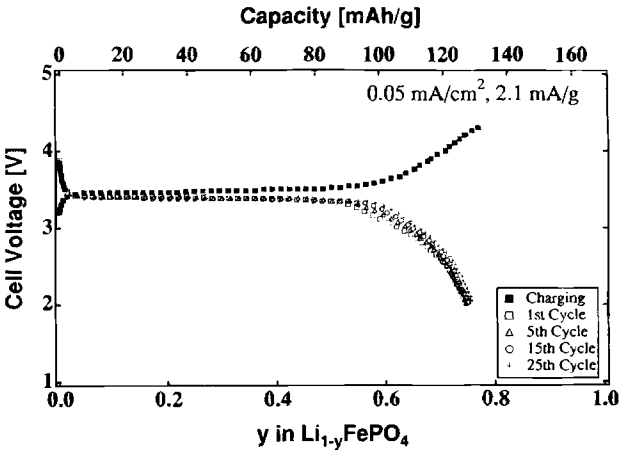

Fig. 2. Discharge/charge curves *vs.* lithium at 2.0 mA/g (0.05 mA/cm²) for $Li_{1-y}FePO_4$.

and the degree of covalence in the bonding. The Madelung electric field raises the electron energies of the cations and lowers those of anions; in an ionic crystal, the Madelung fields are strong enough to overcome the energy required to create the ionic species, and the redox states are antibonding states of primarily cationic origin. Reference to an Fe^{3+}/Fe^{2+} redox energy implies a substantial ionic component to the bonding; and the stronger the Madelung electric field at the cation site, the higher is the Fe^{3+}/Fe^{2+} redox energy. The Madelung sum of coulomb energies can account qualitatively for a lower Fe^{3+}/Fe^{2+} redox energy, and hence a higher V_{oc} *vs.* lithium in $Li_{1-x}FePO_4$ than in $Li_{3+x}Fe_2(PO_4)_3$. In the NASICON framework, the FeO_6 octahedra share no edges with other cation polyhedra, which reduces the cation-cation coulomb repulsions contributing to the Madelung sum, whereas considerable edge sharing occurs in the ordered olivines. The cation-cation repulsive forces distort the hcp anion array of an olivine, as noted above, but the repulsion is not sufficient to screen the reduction by these forces of the total Madelung electric field that raises the Fe^{3+}/Fe^{2+} redox energy above the $(PO_4)^{3-}$ energies. Therefore, the Fe^{3+}/Fe^{2+} level lies lower in the ordered olivine structure.

The $V(x)$ curves for $Li_{1-x}FePO_4$ in Fig. 2 show a voltage that is independent of x over a large range of x, which indicates, by Gibb's phase rule, that the extraction/insertion reactions proceed by the motion of a two-phase interface. To establish the existence and structure of the second phase, a partial chemical delithiation was performed by reacting $LiFePO_4$ with varying amounts NO_2PF_6 in acetonitrile. Chemical delithiation allows XRD patterns to be taken on clean samples. The XRD patterns in Fig. 3 show the emergence and growth of a second phase at the expense of $LiFePO_4$ as more and more lithium is extracted. With total chemical delithiation, the second phase could be identified by both chemical analysis and Rietveld refinement to XRD data to be $FePO_4$. XRD patterns for chemical lithiation of $FePO_4$, Fig. 4, show the emergence and growth of $LiFePO_4$ at the expense of $FePO_4$ on more lithiation. Electrochemical characterization of a cathode made from the $FePO_4$ obtained by total chemical delithiation of $LiFePO_4$ gave the $V(x)$ curves of Fig. 5; they are similar to those of Fig. 2, thus confirming that $FePO_4$ is the second phase that is present on electrochemical extraction of lithium from $LiFePO_4$. Therefore the extraction of lithium from $LiFePO_4$ to charge the cathode may be written as

$$LiFePO_4 - xLi^+ - xe^- \rightarrow xFePO_4 + (1 - x)LiFePO_4$$

and the reaction for the insertion of lithium into $FePO_4$ on discharge as

$$FePO_4 + xLi^+ + xe^- \rightarrow xLiFePO_4 + (1 - x)FePO_4$$

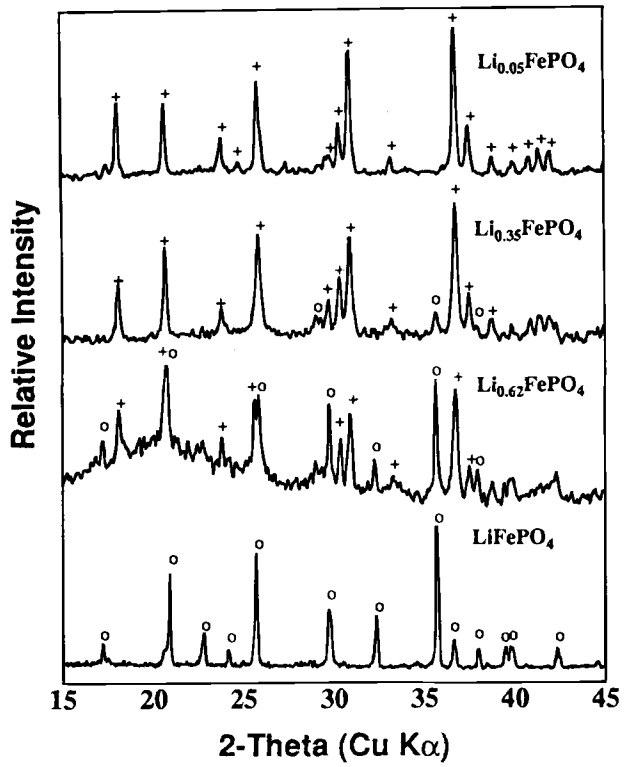

Fig. 3. Chemical delithiation of $LiFePO_4$. XRD patterns showing the emergence and growth of the second phase $FePO_4$.

The excellent reversibility of the cells on repeated cycling is due to the striking similarity of the $LiFePO_4$ and $FePO_4$ structures, which are compared in Fig. 6. $FePO_4$ is isostructural with heterosite, $Fe_{0.65}Mn_{0.35}PO_4$, for which several bond lengths have been refined.[18] The lattice

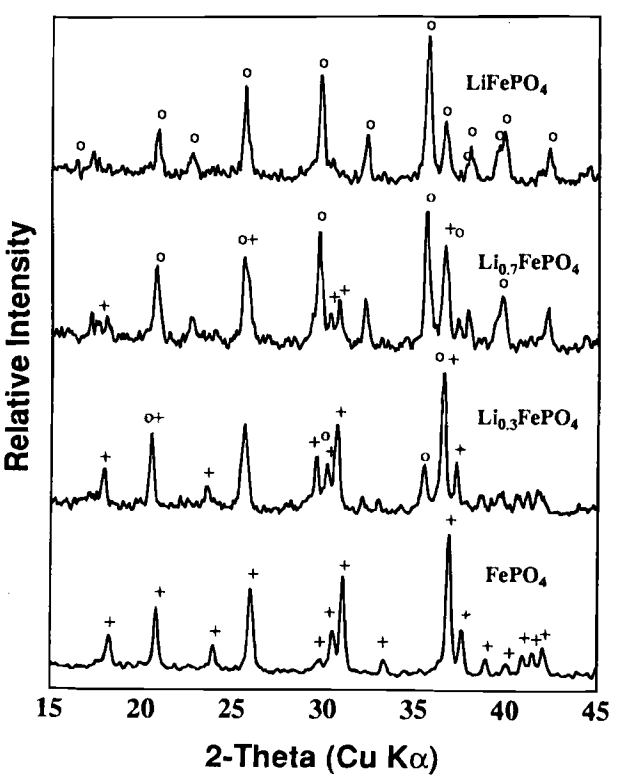

Fig. 4. Chemical lithiation of $FePO_4$. XRD patterns showing the emergence and growth of the second phase $LiFePO_4$.

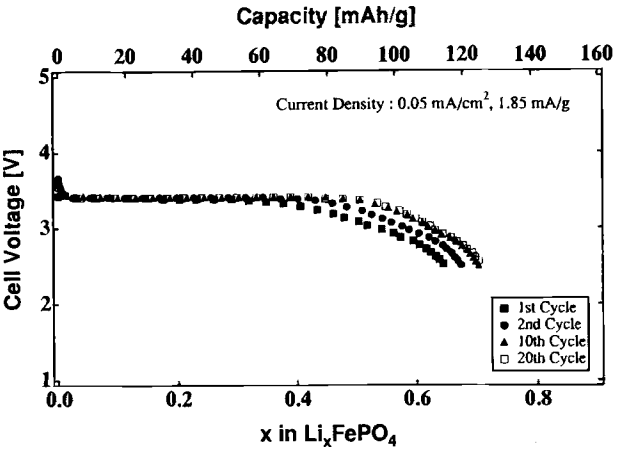

Fig. 5. Discharge/charge curves *vs.* lithium at 2.0 mA/g (0.05 mA/cm²) for Li_xFePO_4.

parameters and the space group of both $LiFePO_4$ and $FePO_4$ phases are listed in Table I; both $LiFePO_4$ and $FePO_4$ have the same space group. On chemical extraction of lithium from $LiFePO_4$, there is a contraction of the *a* and *b* parameters, but a small increase in the *c* parameter. The volume decreases by 6.81% and the density increases by 2.59%. Although the changes in the $FePO_4$ framework are displacive, not diffusional, a first-order transition between $LiFePO_4$ and $FePO_4$ prevents the continuous insertion reaction

$$LiFePO_4 - xLi^+ - xe^- \rightarrow Li_{1-x}FePO_4$$

A first-order transition would seem to require a cooperative elastic deformation of the $FePO_4$ framework. It is therefore of interest that the principal change in the framework on delithiation is a cooperative adjustment of the framework to the coulombic repulsion between the O^{2-}-ion sheet interfacing the delithiated planes.

Insertion of lithium into $FePO_4$ was reversible over the several cycles investigated. Li_xFePO_4 represents a cathode of good capacity, and it contains inexpensive, environmentally benign elements. However, a nearly close-packed hexagonal oxide-ion array that is bonded strongly in three dimensions provides a relatively small free volume for Li^+-ion motion, so the electrode supports only relatively small current densities at room temperature. Nevertheless, increasing the current density does not lower the open-circuit voltage V_{oc}; rather it decreases, reversibly, the cell capacity. Reducing the current restores the capacity. This observation indicates the loss in capacity is a diffusion-limited phenomenon associated with the two-phase character of the insertion process.

As is illustrated schematically in Fig. 7, lithium insertion proceeds from the surface of the particle moving inward behind a two-phase interface, a Li_xFePO_4/$Li_{1-x}FePO_4$ interface in this system. As the lithiation proceeds, the surface area of the interface shrinks. For a constant rate of lithium transport per unit area across the interface, a critical surface area is reached where the rate of total lithium transported across the interface is no longer able to sustain the current; the cell performance becomes diffusion-limited. The higher the current, the greater is the total critical interface area and, hence, the smaller the concentration x of inserted lithium before the cell performance becomes diffusion-limited. On extraction of lithium, the parent phase at the core of the particle grows back toward the particle surface, which is why the parent phase is retained on repeated cycling and the loss in capacity is reversible on lowering the current density delivered by the cell. This loss of capacity is not due to a breaking of the electrical contact between particles as a result of volume changes, a process that is normally irreversible.

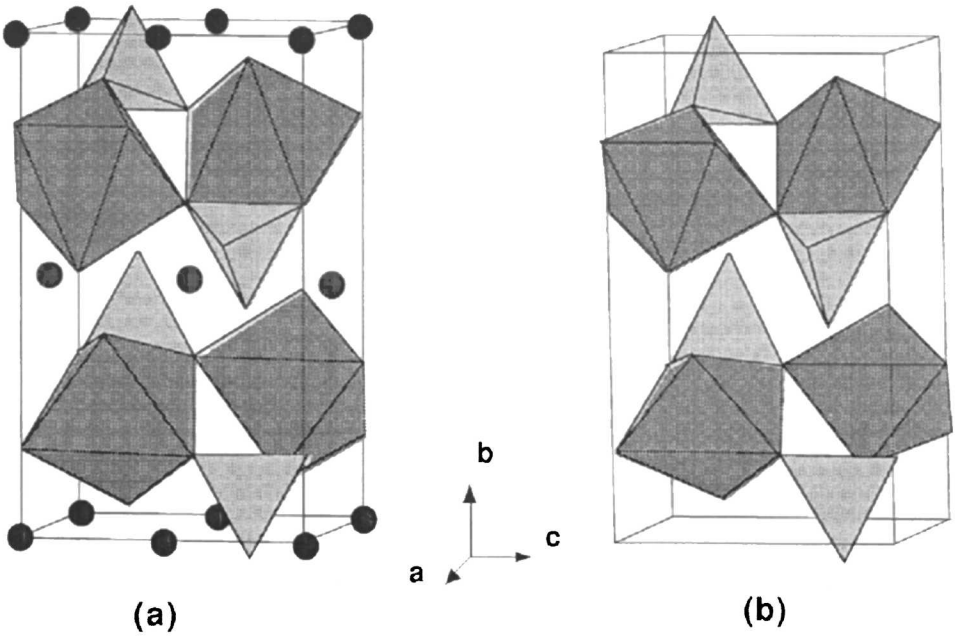

Fig. 6. Crystal structures of (a) $LiFePO_4$ and (b) $FePO_4$.

The thermal stability of the fully charged state of $LiFePO_4$, $FePO_4$, is shown in the TGA curves of Fig. 8. On thermal treatment of $FePO_4$ in nitrogen atmosphere up to 350°C, there was no appreciable change in the weight. A weight loss of 1.6% is observed when the sample was heated up to 500°C. There was very little difference in the TGA curves when the sample was heated in oxygen atmosphere. No appreciable change could be found in the XRD patterns taken after thermal treatment; there was no trace of impurity. Since the $FePO_4$ for these experiments was prepared by treating $LiFePO_4$ with bromine several times in acetonitrile, there could be a small amount of LiBr in the sample even after washing the products several times with acetonitrile, which decomposes at 350°C. The DSC curve shows a small reversible peak at 300°C of unknown origin.

In order to locate the Mn^{3+}/Mn^{2+}, Co^{3+}/Co^{2+}, and Ni^{3+}/Ni^{2+} redox energies with respect to the Fermi energy of lithium, we tried to extract lithium electrochemically from other $LiMPO_4$ compounds with M = Mn, Co, or Ni. Since $LiClO_4$ with 1:1 by volume mixture of PC and DME was used as the electrolyte, the upper voltage limit used in our experiments were 4.3 to 4.4 V. Higher upper voltages resulted in oxidation of the electrolyte, and we could not initiate access to the Mn^{3+}/Mn^{2+}, Co^{3+}/Co^{2+}, and Ni^{3+}/Ni^{2+} redox couples in these compounds. However, we could access the Mn^{3+}/Mn^{2+} couple in the presence of some iron atoms in the structure. Solid-solutions $LiFe_{1-x}Mn_xPO_4$ with x = 0.25, 0.50, and 0.75 were synthesized. Figure 9 shows linear increases of the lattice parameters with increasing Mn content in the structure, in accordance with Vegard's law.

Figure 10a-d show the electrochemical charge and discharge curves for coin-type cells with $LiFe_{1-x}Mn_xPO_4$ (x = 0.25, 0.50, 0.75, and 1.0) as the cathode and lithium as the anode. The charging curve for $LiFe_{0.75}Mn_{0.25}PO_4$, Fig. 10a, shows a small plateau at 4.1 V, which is not very distinguishable in the discharge curve. For $LiFe_{0.5}Mn_{0.5}PO_4$, the charging curve Fig. 10b shows two distinct plateaus of almost equal width, and these plateaus are reproducible on discharge and over repeated cycling. As the Mn content is increased in the structure, the amount of lithium that can be electrochemically extracted by charging decreases as is evident in Fig 10c for $LiFe_{0.25}Mn_{0.75}PO_4$. With all the Fe atoms replaced by Mn atoms as in $LiMnPO_4$, lithium could not be extracted either electrochemically, Fig. 10d, or chemically by reacting with NO_2PF_6 in acetonitrile.

From these observations, we conclude that the Mn^{3+}/Mn^{2+} redox couple in phospho-olivines lies 4.1 eV below the Fermi energy of lithium if the Mn atoms have an Fe atom as a nearest neighbor. Destabilization in the presence of iron of the Mn^{3+}/Mn^{2+} redox couple from over 4.3 to 4.1 eV below the Fermi energy of lithium could reflect the Fe^{3+}-O-Mn^{2+} superexchange interaction; the Mn^{2+} level would be antibonding and the Fe^{3+} level bonding with respect to this interaction. In $LiMPO_4$ with M = Co and Ni, the M^{3+}/M^{2+} redox energies lie well below the highest occupied molecular orbital of our electrolyte, with the Ni^{3+}/Ni^{2+} redox couple lying around 0.6 eV below the Co^{3+}/Co^{2+} redox couple as in the case of the inverse spinels V[LiM]O_4

Table I. The space group and lattice parameters of $LiFePO_4$ and delithiated phase $FePO_4$.

	$LiFePO_4$	$FePO_4$
Space Group	Pb nm	Pb nm
a (Å)	6.008 (3)	5.792 (1)
b (Å)	10.334 (4)	9.821 (1)
c (Å)	4.693 (1)	4.788 (1)
Volume (Å^3)	291.392 (3)	272.357 (1)

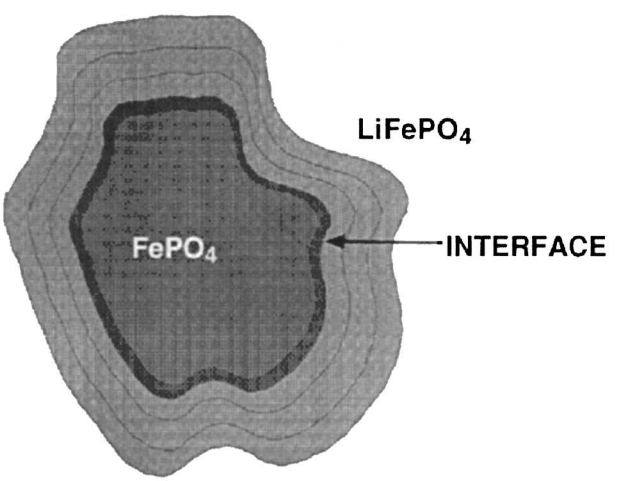

Fig. 7. Schematic representation of the motion of $LiFePO_4/FePO_4$ interface on lithium insertion to a particle of $FePO_4$.

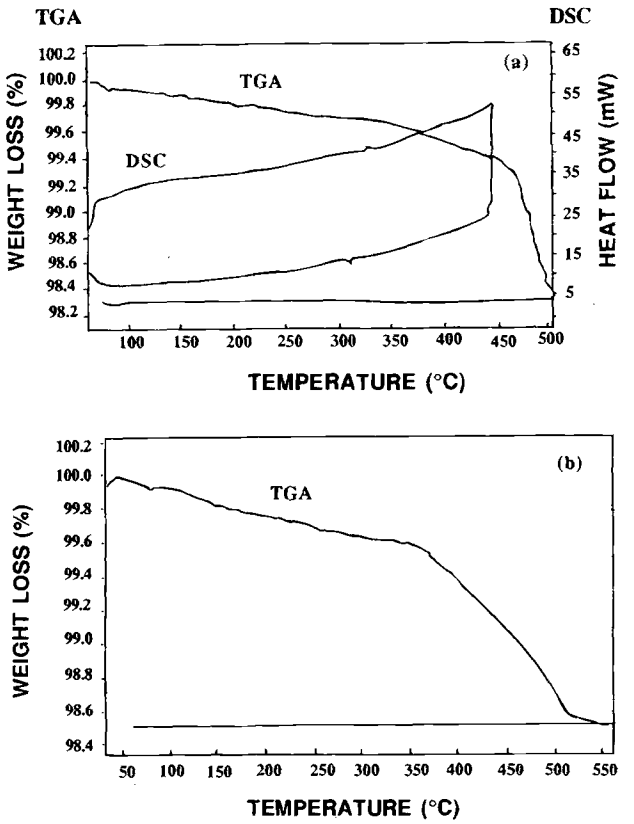

Fig. 8. The thermal stability of delithiated phase $FePO_4$: (a) TGA and DSC curves in nitrogen atmosphere and (b) TGA curve in oxygen atmosphere.

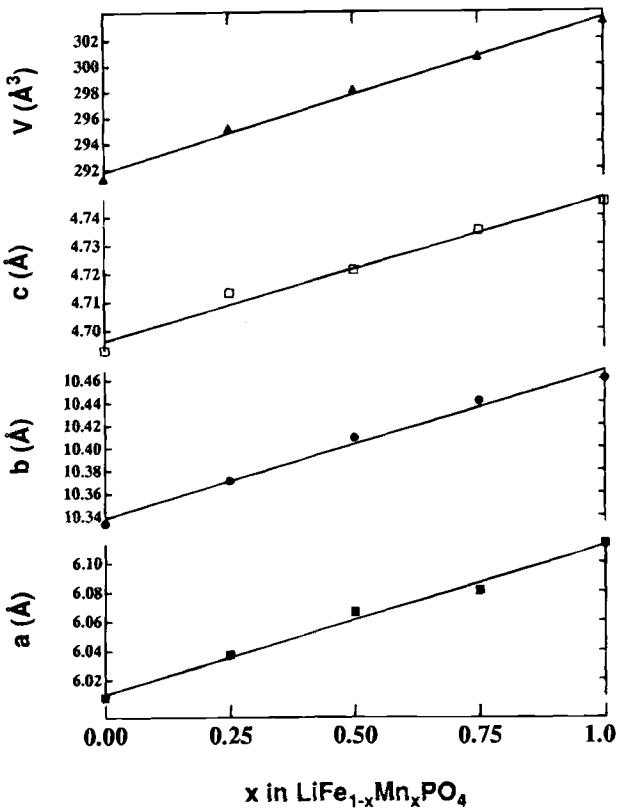

Fig. 9. Variation of lattice parameters of $LiFe_{1-x}Mn_xPO_4$ with increasing Mn content in the structure.

with M = Co or Ni. [19] It appears that the greater covalence of the PO_4 tetrahedron relative to that of the VO_4 tetrahedron not only favors the olivine as against the spinel structure; it also stabilizes the redox couples at the octahedral sites by at least 0.4 eV, lowering the Mn^{3+}/Mn^{2+} couple from 3.7 eV below the lithium-anode Fermi energy in $V[LiMn]O_4$ to 4.1 eV in $LiFe_{0.5}Mn_{0.5}PO_4$. [20]

Conclusion

On extraction of lithium from $LiFePO_4$, a flat closed-circuit voltage (CCV) curve at 0.05 mA/cm² of 3.5 V *vs.* lithium is obtained for the Fe^{3+}/Fe^{2+} redox couple due to the presence of two phases, $LiFePO_4$ and $FePO_4$. These phases belong to the same space group with a variation of the $FePO_4$ host only in the unit-cell parameters. This material is very good for low-power applications; at higher current densities there is a reversible decrease in capacity that, we suggest, is associated with the movement of a two-phase interface, a feature characteristic of cathodes that traverse a two-phase compositional domain in the discharge cycle. The intercalation of only 0.6 Li atom/formula unit of $LiFePO_4$ may be an extrinsic problem since the same $V(x)$ curves are obtained starting with $FePO_4$ and essentially all the lithium can be extracted chemically from $LiFePO_4$.

The deintercalation of lithium from the solid solution $LiFe_{1-x}Mn_xPO_4$ (x = 0 to 1) allows location of the position of the Mn^{3+}/Mn^{2+} redox couple. When x = 0, we get a plateau at 3.5 V; but as the manganese content is increased, a plateau at 4.1 V appears. Maximum charging at 4.1 V is accomplished for x = 0.5. As expected, we observe that the oxidation of Mn^{2+} occurs only after the oxidation of Fe^{2+}. We were unable to take out any lithium from $LiMnPO_4$ while charging up to 4.3 V. Moreover, the width of the 4.1 V plateau decreases with increasing $x >$ 0.5, which suggest that the 4.1 V plateau is associated with the Mn atoms having Fe near neighbors. It appears that the Mn-O-Fe interactions raise the energy of the Mn^{3+}/Mn^{2+} couple and slightly lower the Fe^{3+}/Fe^{2+} couple. We were unable to extract Li from isostructural $LiCoPO_4$ and $LiNiPO_4$ with the electrolyte $LiClO_4$ in PC and DME due to the stability of the Co^{3+}/Co^{2+} and Ni^{3+}/Ni^{2+} couples.

Acknowledgment

We thank the Robert A. Welch Foundation, Houston, Texas, for financial support.

Manuscript submitted Sept. 5, 1996; revised manuscript received Dec. 15, 1996.

The University of Texas at Austin assisted in meeting the publication costs of this article.

REFERENCES

1. M. S. Whittingham, *This Journal*, **123**, 315 (1976).
2. K. Mizushima, P. C. Jones, P. J. Wiseman, and J. B. Goodenough, *Mater. Res. Bull.*, **15**, 783 (1980).
3. M. G. S. R. Thomas, W. I. F. David, and J. B. Goodenough, *ibid.*, **20**, 1137 (1985).
4. T. Ohzuku, M. Kitagawa, and T. Hirai, *This Journal*, **137**, 769 (1990).
5. J. M. Tarascon and D. Guymard, *Electrochim. Acta*, **38**, 1221 (1993).
6. J. R. Dahn, E. W. Fuller, and U. von Sacken, *Solid State Ionics*, **69**, 265 (1994).
7. M. M. Thackeray, P. J. Johnson, L. A. de Piciotto, P. G. Bruce, and J. B. Goodenough, *Mater. Res Bull.*, **19**, 179, (1984).
8. M. M. Thackeray, A. de Kock, M. H. Rossouw, D. Liles, R. Bittihu, and D. Hoge, *This Journal*, **139**, 363, (1992).
9. V. B. Nalbandyan and I. L. Shukaev, *Russ. J. Inorg. Chem*, **32**, 3, (1987)
10. Y. Takeda, K. Nakahara, M. Nishijima, N. Imanashi, O. Yamamoto, M. Takano, and R. Kanno, *Mater. Res. Bull.*, **29**, 659 (1994)
11. A. Le Mehaute, G. Ouvrard, R. Brec, and J. Rouxel, *ibid.*, **12**, 1191 (1977).
12. M. S. Whittingham, *Prog. Solid State Chem.*, **12**, 41 (1978)
13. R. Brec and A. Dugast, *Mater. Res. Bull.*, **15**, 619 (1980).

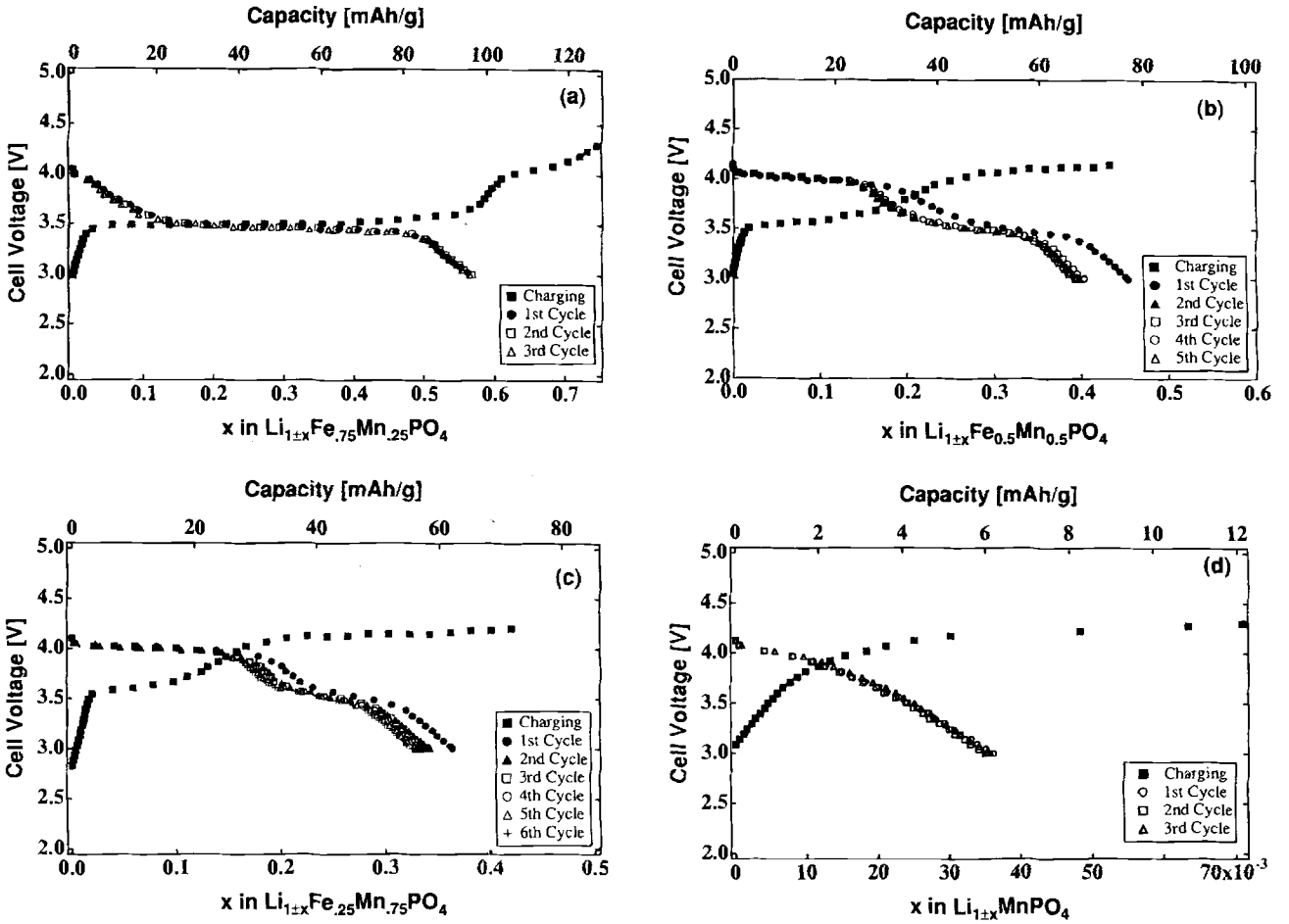

Fig. 10. Discharge/charge curves *vs.* lithium at current densities 2.0 mA/g, (0.05 mA/cm²) for (a) $LiFe_{0.75}Mn_{0.25}PO_4$, (b) $LiFe_{0.5}Mn_{0.5}PO_4$, (c) $LiFe_{0.25}Mn_{0.75}PO_4$, and (d) $LiMnPO_4$.

14. S. Okada, K. S. Nanjandaswamy, A. Manthiram, J. B. Goodenough, H. Ohtsuka, H. Arai, and J. Yamaki, in *Proceedings of 36th International Power Sources Symposium,* p. 110, Cherry Hill, NJ (1994).
15. C. Masquelier, A. K. Padhi, K. S. Nanjandaswamy, and J. B. Goodenough, *J. Solid State Chem.*, Submitted.
16. A. K. Padhi, K. S. Nanjandaswamy, C. Masquelier, and J. B. Goodenough, in *Proceedings of 37th International Power Sources Symposium*, p. 180, Cherry Hill, NJ (1996).
17. G. E. Brown, Ph.D. Thesis, Virginia Polytechnic Institute, Blacksburg, VA (1970).
18. W. Evantoff, R. Martin, and D. R. Peacor, *Am. Min.*, **57**, 45 (1972).
19. G. T. Fey, Wu Li, J. R. Dahn, *This Journal*, **141**, 2279 (1994).
20. A. K. Padhi, W. B. Archibald, K. S. Nanjundaswamy, and J. B. Goodenough, *J. Solid State Chem.*, In press.